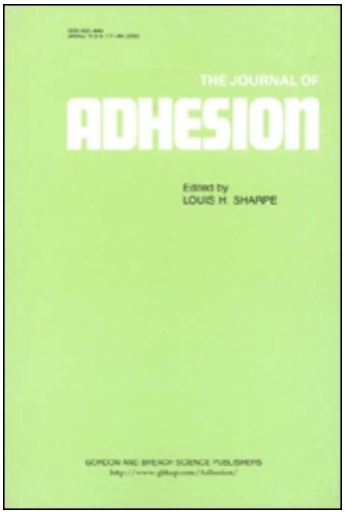

The Journal of Adhesion
Publication details, including instructions for authors and subscription information:
http://www.informaworld.com/smpp/title~content=t713453635

Adhesion Maps Using Scanning Force Microscopy Techniques

P. J. De Pablo[a]; J. Colchero[a]; J. Gomez-Herrero[a]; A. M. Baro[a]; D. M. Schaefer[b]; S. Howell[c]; B. Walsh[c]; R. Reifenberger[c]
[a] Dept. Física de la Materia Condensada, Universidad Autónoma de Madrid, Madrid, Spain [b] Department of Physics, Towson University, Towson, MD, USA [c] Department of Physics, Purdue University, W. Lafayette, Indiana, USA

To cite this Article De Pablo, P. J. , Colchero, J. , Gomez-Herrero, J. , Baro, A. M. , Schaefer, D. M. , Howell, S. , Walsh, B. and Reifenberger, R.(1999) 'Adhesion Maps Using Scanning Force Microscopy Techniques', The Journal of Adhesion, 71: 4, 339 — 356
To link to this Article: DOI: 10.1080/00218469908014547
URL: http://dx.doi.org/10.1080/00218469908014547

J. Adhesion, 1999, Vol. 71, pp. 339–356
Reprints available directly from the publisher
Photocopying permitted by license only

Adhesion Maps Using Scanning Force Microscopy Techniques

P. J. DE PABLO[a], J. COLCHERO[a], J. GOMEZ-HERRERO[a], A. M. BARO[a], D. M. SCHAEFER[b], S. HOWELL[c], B. WALSH[c] and R. REIFENBERGER[c,*]

[a] *Dept. Física de la Materia Condensada, Universidad Autónoma de Madrid, 28049-Madrid, Spain;* [b] *Towson University, Department of Physics, Towson, MD 21234, USA;* [c] *Purdue University, Department of Physics, W. Lafayette, Indiana 47907, USA*

(Received 24 August 1998; In final form 22 July 1999)

A technique has been developed that allows a real-time measurement of the lift-off force required to remove a scanning force microscope tip from a substrate. Both topography and adhesion maps are obtained simultaneously, allowing the correlation between topography and adhesion properties to be studied. Quantitative values of important adhesion parameters can be extracted from these data. A number of examples are given which illustrate the utility of this technique.

Keywords: Microscopic adhesion; spatially resolved adhesion; Atomic Force Microscope (AFM); Scanning Force Microscope (SFM)

I. INTRODUCTION

There is increasing interest in using Scanning Force Microscope (SFM) techniques to measure the adhesion properties of a substrate at the nanometer-length scale. The interest derives from the adhesive forces acting on an SFM tip when touched to a substrate. These adhesive forces can be quantitatively measured by monitoring the deflection of the SFM cantilever. The relevant aspects of such an SFM

*Corresponding author. Tel.: 765-494-3032, Fax: 765-494-0706, e-mail: rr@physics.purdue.edu

experiment are illustrated in Figure 1, which schematically shows the force acting on an SFM cantilever as the surface-to-surface separation between the tip and the substrate is changed. Using this SFM configuration, the force acting on the particle is inferred from the measured deflection of the cantilever with a known spring constant, k.

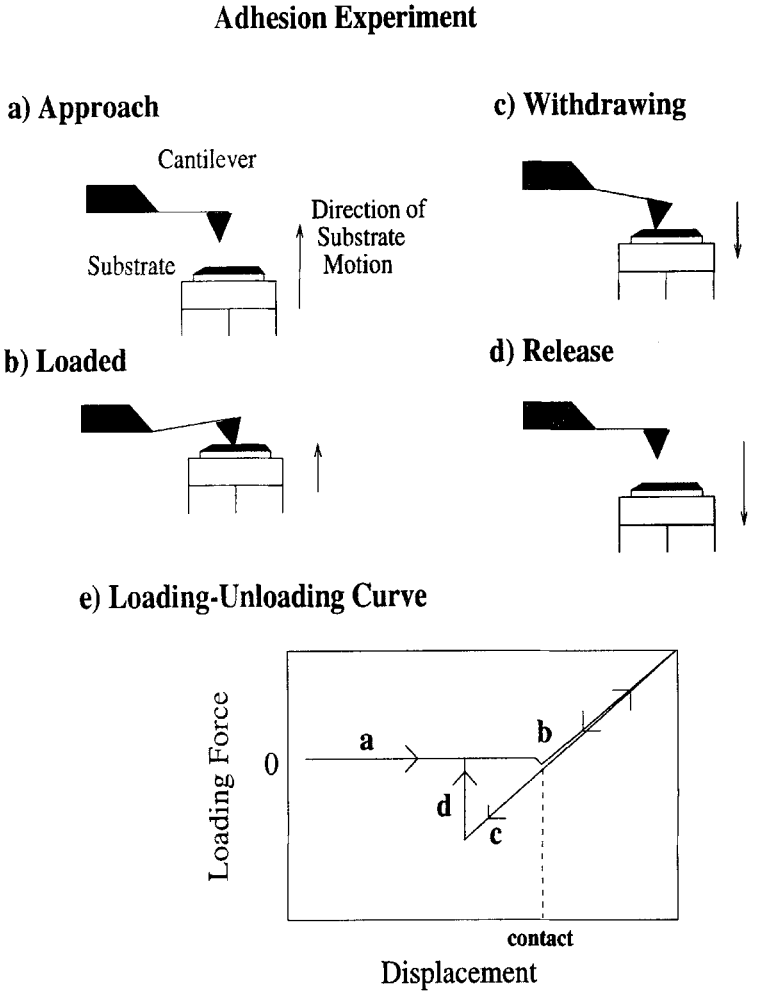

FIGURE 1 Schematic of a force curve in scanning force microscopy (SFM). The idea behind an adhesion map is to plot the variation of the lift off force, measured in segment **d** of the force curve, as a function of position.

Such an experiment displays five important regimes. Initially, the tip is assumed to be sufficiently far from the substrate so as not to be influenced by it. As the surface-to-surface separation distance between the tip and substrate is decreased, any forces acting between the tip and substrate cause a deflection of the cantilever (region "a" of Fig. 1). The distance dependence of this deflection is useful for identifying the origin of the interaction force [1]. When the tip is only a few tens of nanometers from the substrate, an instability arises and the tip jumps into contact with the substrate (region "b" of Fig. 1). After contact is made, a controlled loading and unloading of the tip against the substrate can be performed (region "c" of Fig. 1). Since the maximum applied load can be controlled in a straightforward way, a quantitative determination of the importance of elastic and plastic processes can result. Upon unloading, the adhesive properties of the tip-substrate can be investigated (region "d" of Fig. 1). The work of adhesion as well as the lift-off force (region "e" of Fig. 1) can then be determined.

One major advantage of the SFM technique is that systematic and controlled experiments can be performed as a function of environmental conditions, substrate composition and substrate topography. In this way, important information about the adhesive properties of different tip/substrate systems can be investigated. Recently, by attaching micrometer-size particles to an SFM tip, experiments that characterize the interaction forces acting on the particle as it approaches a substrate have been reported [2–7]. Such experiments are ultimately useful for understanding the adhesion between a particle and a substrate.

As examples of the type of information obtained from such studies, Gady *et al.* [6] have carefully investigated the region of the force curve labeled by "a" in Figure 1. In these experiments, a micron-size polystyrene sphere was affixed to the cantilever. The forces acting on a polystyrene sphere were determined by directly measuring the deflection of the SFM cantilever and using oscillating cantilever techniques to measure the force gradient. Both a van der Waals and localized electrostatic (or "charged patch") [8] contributions to the interaction force were identified. In subsequent studies, a better characterization of the electrostatic contribution to the interaction force was completed, allowing for a quantitative estimate of the charge transfer between the particle and the substrate [1].

Schaefer *et al.*, also studied the adhesive forces by systematically measuring the force required to remove different micrometer-diameter particles from a variety of substrates [5]. In this study, the relative lift-off forces were found to scale consistently with the relative works of adhesion in a manner qualitatively consistent with the predictions of the Johnson, Kendall, Roberts (JKR) theory of adhesion [9]. The absolute magnitude of the lift-off force was found to be smaller than expected. This effect was attributed to the surface roughness of the particle which reduced the contact area between the particle and substrate. Although most of these studies mentioned above have been confined to well-characterized, spherical particles and atomically-flat substrates, the results obtained indicate that the SFM techniques developed are capable of providing useful, quantitative information about particle adhesion that is difficult to ascertain using more conventional techniques.

Most recently, the region of the force curve known as the jump-to-contact (region "b" in Fig. 1) has been studied [10]. The cantilever experiences an increasingly attractive force as the separation distance between the particle and substrate decreases. An instability results at a point where the cantilever can no longer compensate for the interaction force between the particle and the substrate. At this point, a sudden jump to contact of the particle to the substrate occurs. In order to predict the point of instability when jump to contact occurs, it is necessary to know in some detail the spatial dependence of the interaction force which the particle experiences. Measuring the jump-to-contact distance, therefore, provides a further test of the interaction force between particle and substrate. The jump-to-contact region has been analyzed, taking into account the effects of both van der Waals and electrostatic forces on this phenomenon and systematic measurements of the separation distance at which jump to contact occurs were quantitatively analyzed, using reasonable models for the interaction force between the particle and substrate [10].

In what follows, we extend this work by directly measuring the lift-off force as a function of position between an SFM cantilever tip (radius $\sim 10\,\text{nm}$) and a variety of different substrates. A similar approach has been implemented in prior studies using analog techniques [11–13]. Because Digital Signal Processor (DSP) techniques are employed, it is possible to achieve flexible control, allowing quick acquisition of data not possible using analog methods.

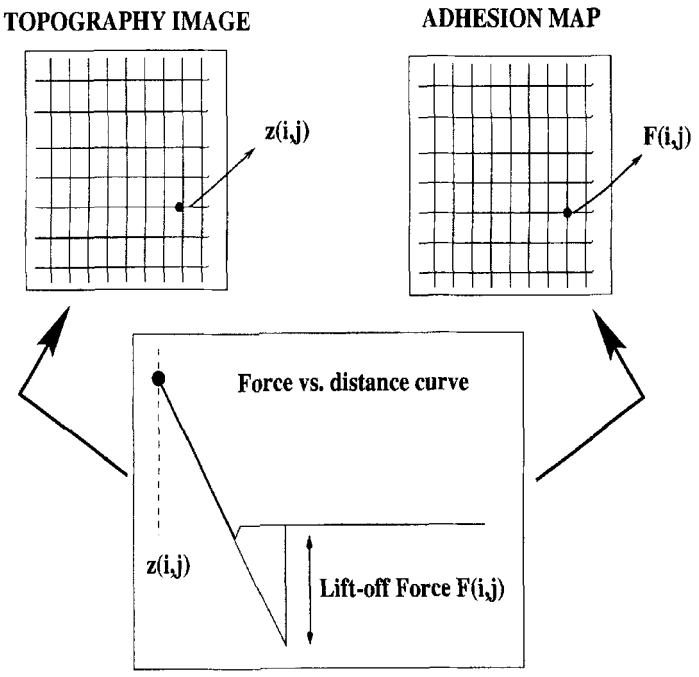

FIGURE 2 Schematic of an adhesion map showing how the topography and adhesion of the tip to the substrate are measured simultaneously.

The basic idea behind an adhesion map is shown in Figure 2 which illustrates how the spatial dependence in the lift-off force and the topography are measured simultaneously during an SFM scan. Because of the large number of data points acquired during each map (typically greater than 10^4), a meaningful statistical analysis of the measured quantities becomes possible. The so-called adhesion maps produced in this way, along with a statistical analysis of the values measured, provide valuable insight into the microscopic variations of the adhesive properties between two objects.

II. EXPERIMENTAL SFM CONSIDERATIONS

We have used two different SFM heads to perform the experiments presented here. The first SFM is a commercially-available instrument

from NanoTec^{TM} which features a modular design, easy adjustment of the optical system, top view of the SFM scanning region which makes it easy for optical microscope inspection, low thermal drift and a humidity-controlled system. The scanning range is up to $50\,\mu m \times 50\,\mu m$. The cantilever deflection was monitored by a laser beam deflection system. The system uses a large piezo tube to minimize hysteresis effects. SiN_3 pyramidal cantilevers from Olympus ($k \simeq 0.4\,nN/nm$) were used in this system.

The second system has been described previously [14, 15] and is mounted in a small stainless steel vacuum chamber, allowing for control of environmental conditions. To avoid problems associated with adsorbed water, the system was repeatedly pumped out to pressures of 20 mTorr, followed by a backfill with dry nitrogen gas. To study the effects of ambient conditions on adhesion, the system could also be vented to atmosphere. Si ultra-cantilevers from Park Scientific ($k \simeq 2.0\,nN/nm$) were used in this system.

Several procedures have been followed during these adhesion studies. Briefly, detection of the SFM cantilever displacement is performed using laser deflection techniques. Calibration of the cantilever spring constant is performed by measuring the resonance frequency [16]. In the SFM system mounted inside the stainless steel chamber, a second laser deflection system is used to monitor the motion of the sample piezoelectric tube. This is critical for eliminating piezoelectric nonlinearities and creep when performing force measurements.

Both SFMs were controlled by a PC-based NanoTec^{TM} control unit. This system of hardware and software controls all aspects of data acquisition, processing and feedback and is now a standard feature of the NanoTec^{TM} software package. The core of the system is a Digital Signal Processor (DSP) with 4 simultaneous ADC/DAC channels, each with 16-bit accuracy. The DAC outputs drive a high voltage amplifier unit which provides the scanning signals. Control and data signals are input through the ADC channels. Scanning and force measurements are performed in real time under the execution of a C program which resides in the DSP memory.

Simultaneous, real time images of the sample topography and lift-off force were performed in the so-called "jumping mode" (see Fig. 3) [17]. This figure shows the motion of the tip as a function of time along (a) the x-axis and (b) the z-axis. In addition, (c) the cantilever

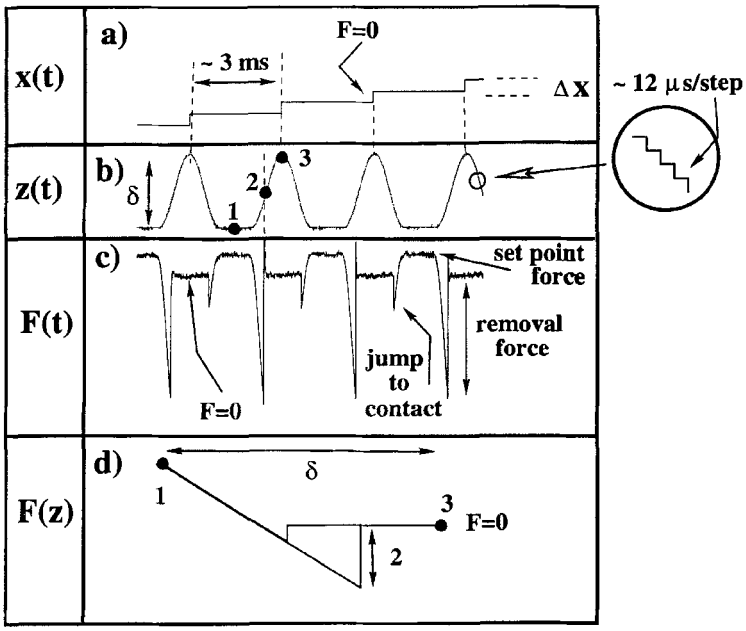

FIGURE 3 Oscilloscope traces showing (a) the position of the sample along the x-axis as a function of time; (b) the position of the sample along the z-axis as a function of time; (c) the normal force applied to the substrate by the tip as a function of time and (d) a schematic of the resulting force curve obtained during one cycle of the z-piezo.

deflection recorded as the tip is moved along the z-axis is also illustrated. In (d), a schematic of the resulting force curve is shown.

The SFM tip is first brought into contact with the sample during the coarse approach, under feedback control, until the setpoint cantilever displacement is achieved. The feedback is then disabled, and a ramp to the z-piezo (which controls the position of the sample with respect to the tip) is applied, withdrawing the sample by a prescribed amount. With the tip in this position, the topography and adhesion maps can then be performed. At each point in the image, the control unit ramps the z-piezo voltage to move the sample through a given distance δ *towards* the tip. This brings the tip into contact with the sample. The cantilever displacement is monitored during this process, providing the approach segment of the force curve. When the ramp is complete, the feedback is then enabled for a short time (typically 1 ms) and its output is stored as the topographic height. The feedback is then

disabled, and an inverse ramp is applied to the z-piezo, withdrawing the tip from the sample. Again, the cantilever deflection is monitored, providing the "withdrawal" portion of the force curve.

When the largest z value is reached (*i.e.*, the maximum tip-sample distance), a voltage step is applied to the x-piezo and the tip is quickly moved parallel to the surface. This allows motion without lateral force, and is similar to a "tapping mode scan". This process is repeated for all points in the image, providing topographic and force curve data at each point. The entire force curve at each point is, however, not stored in memory. Storing such data would significantly slow the scanning speed and require large amounts of memory. After each force curve has been completed, the relevant local parameters (such as lift-off force or elastic modulus) are extracted from the force curve, and only these values are stored in memory. Following this approach, an entire adhesion map consisting of 256 by 256 data points takes about 10 minutes to complete.

In order to perform quantitative adhesion maps in real time, it was important to optimize the system's performance. Since the modulation of the z-position during force curves is typically performed by ramping at a frequency of 1 kHz, resonant frequencies can easily be excited in the system. In order to prevent these excitations, a look-up table with a sine-wave ramp was generated by the DSP and then applied to the z piezoelectric driver. The frequency of the sinusoidal ramp was chosen away from the resonance frequencies of the system.

III. FACTORS INFLUENCING ADHESION

It is useful to review some of the basic factors influencing adhesion between a point-probe, similar to an SFM tip, and a substrate. When two surfaces are brought into contact, it is convenient to describe the lift-off force (or adhesion force) in terms of surface energies rather than surface forces. The advantages of this approach have been discussed elsewhere [18].

The tip-sample system under consideration here (see Fig. 4) can be characterized as a tip with radius, R_{tip}, and surface energy, γ_{tip}, and a substrate with local radius of curvature, R_{sub}, and surface energy, γ_{sub}. The force required to cause separation of the tip from the substrate depends on these four parameters. To separate each unit area

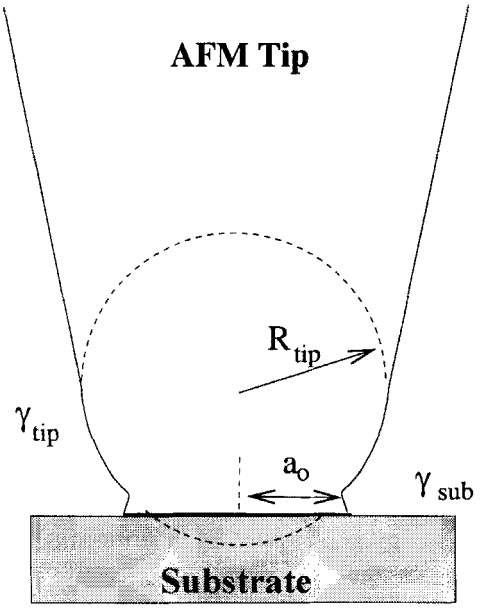

FIGURE 4 A schematic diagram of the JKR model for the adhesion of an SFM tip of radius, R_{tip}, on a perfectly-flat substrate. Because of adhesion, a contact radius, a_o, results which can be estimated from the surface energies of the tip (γ_{tip}) and substrate (γ_{sub}). If the substrate has a local radius of curvature, then an effective tip radius must be defined (see Eq. (2) in the text).

in contact involves an amount of energy given by $\Delta\gamma = \gamma_{tip} + \gamma_{sub} - \gamma_{tip,sub}$, where $\gamma_{tip,sub}$ is defined as the interfacial energy. The interfacial energy, $\gamma_{tip,sub}$, is a system-dependent quantity.

An estimate of the lift-off force can be obtained by equating the mechanical work required to separate the two objects to $\Delta\gamma$. If we deal with reversible systems assumed to be free of contaminants, the force required to separate the two objects is often discussed within the Johnson, Kendall, Roberts (JKR) theory [9] which calculates that the lift-off force is given by

$$F_{\text{lift-off}} = 1.5\pi\, R_{\text{eff}}\, \Delta\gamma \tag{1}$$

where

$$\frac{1}{R_{\text{eff}}} = \frac{1}{R_{\text{tip}}} + \frac{1}{R_{\text{sub}}}. \tag{2}$$

Values for R_{eff} range between a lower limit near zero (appropriate when R_{sub} for a substrate has features small compared with the tip radius) and an upper limit of R_{tip} (appropriate when R_{sub} approaches infinity, *i.e.*, for a substrate that is very flat).

The JKR model is useful because it nicely separates out two important contributions to adhesion. The lift-off force depends on the product of two terms: one describes the surface properties of both the tip and substrate ($\Delta\gamma$) and the other describes the local geometry of the tip/substrate (R_{eff}). For experiments performed on clean surfaces with an SFM tip, it is reasonable to assume that $\Delta\gamma$ is roughly independent of position. This assumption, in turn, requires that any observed spatial variation in adhesion be attributed to spatial variations in R_{eff}. It, therefore, becomes important to understand how R_{eff} is influenced by substrates having different roughness characteristics.

Within this context it is useful to consider how R_{eff} varies as a function of R_{sub} (see Eq. (2)) as shown by the solid line in Figure 5. Here we normalize both R_{eff} and R_{sub} by the tip radius, R_{tip}, since for a given experiment R_{tip} is usually fixed. It follows that, for a given substrate roughness, there will be a corresponding distribution of R_{sub} which determines the adhesion of the tip to the substrate.

For smooth substrates, the roughness of the substrate (characterized by statistically measuring a distribution, $R_{\text{sub}}/R_{\text{tip}}$, shown schematically in Fig. 5) will be centered around an average value of $R_{\text{sub}}/R_{\text{tip}}$ considerably greater than 1. The width of this distribution, indicated as $2\sigma_a$ in Figure 5, will give rise to only a narrow distribution in R_{eff}. For flat substrates, variations in $F_{\text{lift-off}}$ will be dominated by a variation in $\Delta\gamma$ since, in this limit, R_{eff} becomes insensitive to variations in R_{sub}. In this case, one might expect a histogram of the measured $F_{\text{lift-off}}$ to display a distribution with a dispersion that reflects variations in $\Delta\gamma$ across the substrate.

In the limit of rough substrates ($R_{\text{sub}}/R_{\text{tip}} < 1$), a distribution of $R_{\text{sub}}/R_{\text{tip}}$ will be centered around an average value of $R_{\text{sub}}/R_{\text{tip}}$ less than 1. The width of this distribution, indicated schematically as $2\sigma_r$ in Figure 5, will give rise to a correspondingly-broad distribution in R_{eff}. In this limit, R_{eff} is dominated by variations in R_{sub} and a histogram of the measured $F_{\text{lift-off}}$ will display a distribution with a dispersion that is dominated by variations in surface roughness rather than by variations in $\Delta\gamma$ across the substrate.

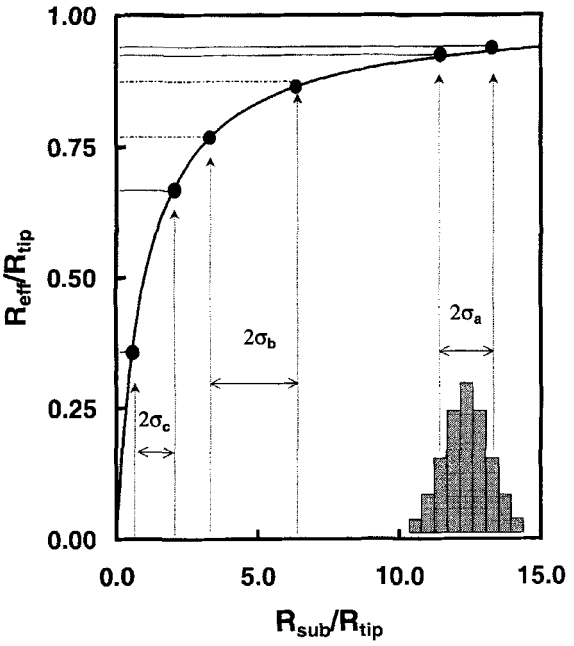

FIGURE 5 A plot of R_{eff}/R_{tip} as a function of R_{sub}/R_{tip}, according to the JKR model of adhesion. The solid line shows how, for a fixed tip radius, the effective radius will vary as a function of surface roughness. The histograms schematically illustrate how variations in surface roughness (R_{sub}) influence the spatial variation in adhesion. The histogram labeled $2\sigma_a$ is for smooth substrates, while that labeled $2\sigma_c$ is for rough substrates.

For the intermediate case of roughness, indicated schematically by $2\sigma_b$ in Figure 5, variations in R_{sub} will cause a non-linear variation in R_{eff}. This is due to the non-linear dependence between R_{sub} and R_{eff} in this regime. In turn, it is expected that, in this regime, a distribution of $F_{lift-off}$ from the substrate will acquire an asymmetric character, with substantially more dispersion observed below the mean value of $F_{lift-off}$ than above.

Qualitatively, the roughness of a substrate can be estimated from the dispersion of a histogram of measured heights obtained from an SFM topographical image. If the average lift-off force is weakly dependent on surface roughness (as characterized by the dispersion of heights from an SFM histogram), then the measured lift-off forces are likely determined by the tip radius and variations in $\Delta\gamma$. If there is a correlation between average lift-off force and surface roughness,

then the average lift-off force is probably dominated by geometrical surface effects (R_{eff}).

It is useful to estimate the lower limit for the length scale of relevant variations in the local radius of curvature of the substrate. This lower limit is roughly set by the contact radius, a_o, that develops when a tip of radius, R, comes into contact with a flat substrate. A well-known consequence of the JKR theory is the prediction of such a contact radius, a_o, at zero applied load. According to the JKR model [9]

$$a_o = \left(\frac{6\pi R^2 \Delta\gamma}{K} \right)^{\frac{1}{3}}. \tag{3}$$

The parameter K includes the elastic properties of the sphere and substrate and is specified by

$$K = \frac{4}{3} \left(\frac{1 - \nu_{\text{tip}}^2}{E_{\text{tip}}} + \frac{1 - \nu_{\text{sub}}^2}{E_{\text{sub}}} \right)^{-1}. \tag{4}$$

Here, ν_{tip} and ν_{sub} are the Poisson's ratios of the tip and substrate, respectively, and E_{sub} and E_{tip} are the Young's moduli for the substrate and the tip. For the materials used in this study (SiO_2, Au, HOPG), estimates of a_o in the 1–2 nm range are expected.

IV. RESULTS

Adhesion maps were performed on a variety of different materials to explore fully the capabilities of the adhesion mapping technique. In these initial studies, emphasis was placed on substrates which can be controllably roughened in order to learn whether any of the trends discussed above can be observed.

A. Adhesion to Thin Au Films Thermally Evaporated onto Glass

Gold was thermally evaporated onto a clean glass slide in such a way as to form two separate electrical contact pads, 60 nm thick and separated by $\sim 10\,\mu$m. A nominal 30 nm thick Au film was then

evaporated through a mask positioned at right angles to these contact pads to form a thin electrical connection (*i.e.*, a bridge) between the two contact pads. This fabrication technique has the advantage that two chemically-identical surfaces (in this case Au) can be prepared with different thicknesses. Since the roughness of a film tends to increase with thickness, various regimes of substrate roughness can be obtained on one sample.

Both topography and adhesion maps were obtained in the region spanning the Au bridge as shown in Figure 6. Figure 7(a) provides an analysis of the surface topography by plotting height histograms taken from the SFM images for the three features of interest - the glass substrate, the Au bridge and the Au contact pad. An examination of Figure 7(a) shows that the glass substrate is considerably smoother (smaller full-width at half-maximum) than either the Au contact pad or the Au bridge. The greater spread in heights measured from the Au contact pad is evident and indicates a greater roughness characterizing this thicker part of the Au substrate. From a calculation of the width (*i.e.*, standard deviation) of these histograms, the roughness of the Au film increases in rough proportion to its thickness, as expected.

It is interesting to see how the surface roughness of the Au substrate influences adhesion. An analysis of the relevant adhesion maps

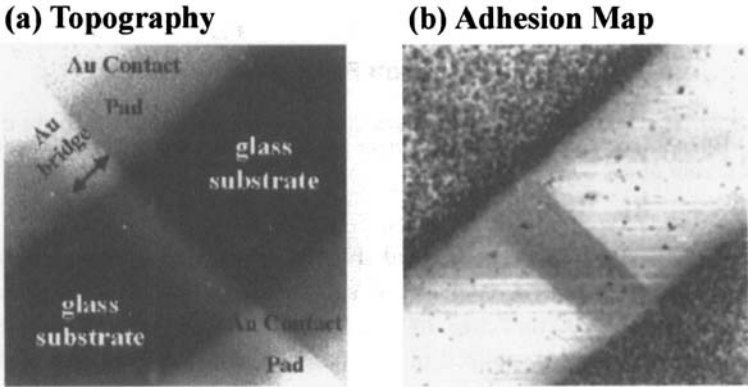

FIGURE 6 (a) A 10 μm by 10 μm SFM topographic scan (jump mode) of two Au contact pads spanned by a thin Au bridge supported on a glass substrate. In (b), an adhesion map of the same region. A mapping algorithm was used such that a lighter gray-scale implies a larger adhesion force.

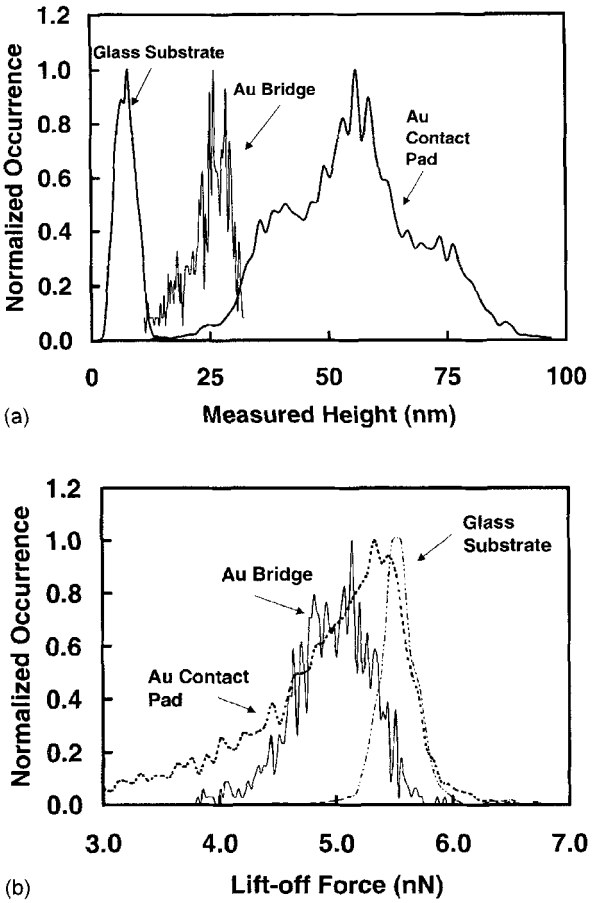

FIGURE 7 A histogram from the images shown in Figure 4 displaying (a) the distribution of heights and (b) the distribution of lift-off force measured for the three relevant regions of the Au/glass sample.

permits this study to be performed. Figure 7(b) shows a histogram of lift-off forces measured on the glass substrate, the Au bridge and the Au substrate. For the case of the glass substrate, the dispersion in adhesion is small, reflecting the smooth character of the glass substrate. The adhesion histograms for the Au substrates show a different behavior. While the average adhesion (*i.e.*, the mean lift-off force) is roughly the same for both the smooth (bridge) and rough (contact pad) regions of the Au substrate, the lift-off forces disperses

asymetrically *to lower values* as the Au substrate becomes rougher. These results are in qualitative agreement with expectations surrounding the discussion of Figure 5.

In addition, another feature in adhesion can be observed from the adhesion maps in Figure 6. From the topographic images, there is clear evidence of particulate contamination, with observed features having dimensions of ~ 90 nm in apparent diameter and ~ 16 nm in height. The adhesion maps also reveal these features, indicating a lowering of adhesion when the tip is in contact with the particles. This observation provides clear evidence for a local decrease in adhesion due to particulate contamination on the glass substrate. While this effect can be, in part, attributed to differences in surface free energies, the major contribution to the reduction in lift-off force is believed to come from modifications of the parameter R_{eff} described in Eq. (2) above.

B. Adhesion to an Argon-ion-sputtered HOPG Substrate

It is clear that both topography and chemistry play an important role in determining the shape of an adhesion map. In particular, the details of the roughening of a surface can have important effects. Highly oriented pyrolitic graphite (HOPG) is ideal to illustrate this point because it is comprised of weakly-interacting sheets of graphite that are atomically flat over large regions. Furthermore, due to the bonding of the carbon atoms to form graphitic sheets, the surface of flat HOPG is known to be unreactive. If the HOPG surface is roughened, the adhesion properties might chemically change, since various chemical reactions could be enhanced by roughening. This system can be contrasted to the non-directional nature of bonding between Au atoms studied above. In addition, the nature of the roughening is different for a planar material like HOPG from that for a metallic substrate like Au. Roughened HOPG will have a surface that is characterized by the formation of pits (concave-up features), [19] rather than concave-down features that are found on metal surfaces like Au.

The JKR model does not analyze the case of a pitted surface explicitly but, qualitatively, one would expect an increase in adhesion as the radius of curvature of a pit becomes comparable with the radius of an SFM tip. Thus, pitted surfaces should show an increase in adhesion

as the surface becomes rougher, a prediction opposite to that expected from the JKR model.

To check out this situation, a roughened sample of HOPG was prepared to study the change in adhesion due to surface roughness. A freshly-cleaved HOPG sample was masked in such a way so as to expose approximately one-half of the surface to an argon-ion discharge for approximately 10 minutes at an argon pressure of $\sim 10^{-3}$ Torr, with the sample biased at a potential of 1000 V with respect to ground. Three separate regions across the boundary demarcating that part of the surface completely exposed to the discharge and that part of the surface covered by a mask were then investigated both in the topography and adhesion map modes. The results are given in Figure 8 which shows three maps of both the topography

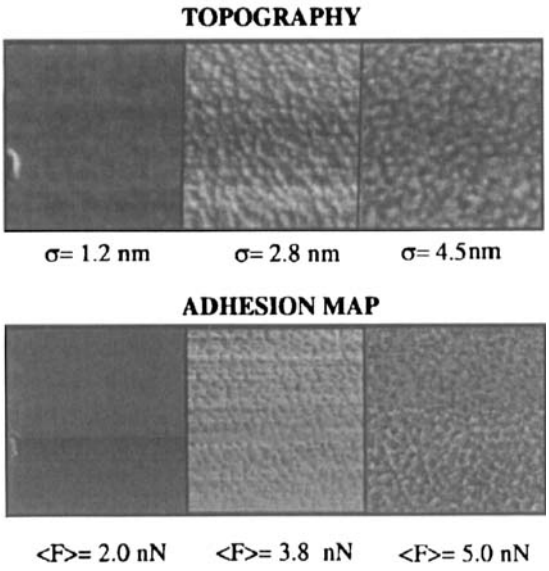

FIGURE 8 Three images, each spanning different 1 μm × 1 μm regions of an HOPG surface exposed to an argon-ion discharge for 10 minutes. Both topography (top sequence) and adhesion maps (bottom sequence) are illustrated. A mapping algorithm was used such that a lighter gray-scale implies a larger adhesion force. Quantitative values for the roughness (calculated from the standard deviation of the topographic image (σ)) and the average lift-off force ($\langle F \rangle$) (acquired from the adhesion map) are listed. A quantitative correlation between substrate roughness and adhesion can be established in this way.

and adhesion near the interface region. A histogram analysis of the images allows a quantitative determination of the roughness by measuring the standard deviation (σ) in topography and the average lift-off force ($\langle F \rangle$) from the adhesion map. These values are listed under each of the three images. A correlation between increasing roughness and the average lift-off force is evident. The correlation of increasing lift-off force with rougher samples is consistent with the lift-off behavior expected for rough pitted samples as discussed above.

V. CONCLUSIONS

Using the NanoTec^{TM} system, we have converted two existing SFMs to acquire simultaneously both topographic and adhesion maps. This was accomplished by implementing only software changes in the Digital Signal Processor (DSP) code. No changes to existing hardware were required. Using these DSP-based techniques, a vast improvement in data acquisition speed over previous analog techniques [11–13] has been obtained.

In this study, the utility of adhesion maps was illustrated by studying different substrates which included Au thin films on glass and an argon-ion-sputtered HOPG substrate. From these studies, geometrical aspects of adhesion have been demonstrated. For the case of Au, we find that the adhesion maps are in agreement with the expectations of a standard theory of adhesion like the JKR model. For the case of HOPG, the surface is pitted and the adhesion is found to increase as the surface is roughened.

Using this DSP-based technique, we expect that adhesion mapping will become a routine characterization tool in the study of surfaces using Scanning Probe Microscope techniques.

Acknowledgments

The authors have benefited from many helpful comments from both D. Rimai and B. Gady of Eastman Kodak Co. The work in Madrid was supported by project CICYT PB95-0169. The work at Purdue was partially funded by the Office Imaging Division of Eastman Kodak.

References

[1] Gady, B., Reifenberger, R., Rimai, D. S. and DeMejo, L. P., *Langmuir* **13**, 2533 (1997).
[2] Schaefer, D. M., Carpenter, M., Reifenberger, R., De Mejo, L. P. and Rimai, D. S., *J. Adhesion Sci. Technol.* **8**, 197 (1994).
[3] Mizes, H. A., *J. Adhes. Sci. Technol.* **8**, 937 (1994).
[4] Ott, M. L. and Mizes, H. A., *Colloids Surf. A* **87**, 245 (1994).
[5] Schaefer, D. M., Carpenter, M., Gady, B., Reifenberger, R., DeMejo, L. P. and Rimai, D. S., *J. Adhesion Sci. Technol.* **9**, 1049 (1995).
[6] Gady, B., Schleef, D., Reifenberger, R., Rimai, D. S. and DeMejo, L. P., *Phys. Rev. B* **53**, 8065 (1996).
[7] Colchero, J., Storch, A., Luna, M., Gomez, J. and Baro, A. M., *Langmuir* **14**, 2230 (1998).
[8] Hays, D. A., "Adhesion of charged particles", In: *Fundamentals of Adhesion and Interfaces*, Rimai, D. S., DeMejo, L. P. and Mittal, K. L., Eds. (VSP, Utrecht, 1995), pp. 61–71.
[9] Johnson, K. L., Kendall, K. and Roberts, A. D., *Proc. R. Soc. London* **A324**, 301 (1971).
[10] Gady, B., Schleef, D., Reifenberger, R. and Rimai, D. S., *J. Adhesion* **67**, 291 (1998).
[11] Koleske, D. D., Lee, G. U., Gans, B. I., Lee, K. P., DiLella, D. P., Wahl, K. J., Barger, W. R., Whitman, L. J. and Colton, R. J., *Rev. Sci. Instrum.* **66**, 4566 (1995).
[12] van der Werf, K. O., Putman, C. A. J., de Grooth, B. G. and Greve, J., *Appl. Phys. Lett.* **65**, 1195 (1994).
[13] Rosa, A., Weilandt, E., Hild, S. and Marti, O., *Meas. Sci. Technol.* **8**, 1 (1997).
[14] Mahoney, W., Schaefer, D. M., Patil, A., Andres, R. P. and Reifenberger, R., *Surf. Sci.* **316**, 383 (1994).
[15] Schaefer, D. M., Andres, R. P. and Reifenberger, R., *Phys. Rev.* B **51**, 5322 (1995).
[16] Cleveland, J. P., Manne, S., Bocek, D. and Hansma, P. K., *Rev. Sci. Instrum.* **64**, 403 (1993).
[17] de Pablo, P. J., Colchero, J., Gomez-Herrero, J. and Baro, A. M., *Appl. Phys. Lett.* **73**, 3300 (1998).
[18] Cohen, S. R., *Ultramicroscopy* **42–44**, 66 (1992).
[19] Chang, H. and Bard, A. J., *J. Amer. Chem. Soc.* **112**, 4598 (1990).